Chapter 3
Flow Cytometry on a Chip

Peter Kiesel, Joerg Martini, Michael I. Recht, Marshall W. Bern, Noble M. Johnson, and Malte Huck

Abstract Flow cytometers are indispensable tools in medical research and clinical diagnostics for medical treatment, such as in diagnosing cancer, AIDS, and infectious diseases. The cost, complexity, and size of existing flow cytometers preclude their use in point-of-care (POC) diagnostics, doctor's offices, small clinics, on-site water monitoring, agriculture/veterinary diagnostics, and rapidly deployable biothreat detection. Here, we present a fundamentally new design for a flow cytometer for the POC that delivers high effective sensitivity without complex optics or bulky, expensive light sources. The enabling technology is spatially modulated emission, which utilizes the relative motion between fluorescing bioparticles and a selectively patterned environment to produce time-modulated signals that can be analyzed with real-time correlation techniques.

3.1 Flow Cytometry

3.1.1 Introduction

Flow cytometers are indispensable tools in medical research and clinical diagnostics for medical treatment, such as in diagnosing cancer, AIDS, and infectious diseases [1]. Chemical and physical information are obtained from functionalized microbeads or bioparticles, for example, cells, viruses, or subcellular complexes, as they are transported in a fluid stream [2]. Conventional flow cytometers can analyze microparticles at rates of ∼50,000 per second [3] and allow for extremely sensitive measurement of particle-associated probes (<100 fluorophores per particle) [2].

P. Kiesel (✉) · J. Martini · M.I. Recht · M.W. Bern · N.M. Johnson · M. Huck
PARC (Palo Alto Research Center Incorporated), 3333 Coyote Hill Rd., Palo Alto, CA 94304, USA
e-mail: Peter.Kiesel@parc.com

D. Issadore and R.M. Westervelt (eds.), *Point-of-Care Diagnostics on a Chip*, Biological and Medical Physics, Biomedical Engineering,
DOI 10.1007/978-3-642-29268-2_3,

Higher analysis rates are limited by detector sensitivity, data acquisition electronics, and cell coincidences. The stochastic arrival of particles in the detection volume limits their concentration to avoid an intolerable number of coincidences.

The cost, complexity, and size of existing flow cytometers preclude their use in point-of-care (POC) diagnostics, doctor's offices, small clinics, on-site water monitoring, agriculture/veterinary diagnostics, and rapidly deployable biothreat detection. The conventional design of flow cytometers is not readily extendable to applications where high performance, robustness, compactness, low cost, and ease of use are required in a single instrument. To date, all fluorescence-based flow cytometers employ the same basic optical configuration, namely, intense illumination of the bioparticle as it speeds through a highly localized light spot, generally generated by a laser [2, 4], an elaborate arrangement of precision optics, and sensitive detectors to record fluorescence and scattered light.

The excitation region covers usually the lateral width of the flow channel and expands some tens of micrometers along the flow direction. A number of commercially available flow cytometers use multiple excitation sources, each focused on a well-defined location or region separate from the others.

The detection region(s) in flow cytometers are commonly defined by – not necessarily diffraction limited – confocal light collection optics with high numerical aperture lenses. Light emitted from each source's region is typically analyzed with a series of dichroic beam splitters, filters, and photomultiplier tubes (PMTs) in order to detect and distinguish differently stained particles including those that simultaneously carry multiple dyes.

The exciting light spot, the detection area, and the particle stream need to reliably overlap in any flow cytometer. Therefore, the size, position, and flow speed of the particle stream need to be accurately controlled, which is typically realized by hydrodynamic focusing. A common implementation of flow focusing is the use of sheath flow, where buffer liquid surrounds the analyte and thereby effectively dilutes the sample, lines up the particles, prevents channel clogging, and maintains clean channel walls. However, the sheath-flow flux can be thousands of times higher than the analyte flux. Therefore, the necessity for large amounts of sheath liquid and waste makes the use of sheath flow impractical for POC testing.

In sheath-flow systems, particles travel at a speed of up to several meters per second resulting in transit times of microseconds. This requires the use of expensive, high-power, low-noise lasers and high-speed data systems, which increases the cost and power requirements of a flow cytometer. In addition, since the detection region is small and the objects traverse it rapidly, such flow cytometers have serious signal-to-noise ratio (SNR) limitations for weakly fluorescing cells. These limitations become more acute if multiple targets must be characterized and distinguished for counting or sorting.

A major cost associated with the use of flow cytometers applied for clinical diagnostics applications is the cost of reagents (e.g., antibodies and conjugated dyes). There are two ways to reduce the amount of consumables: first, one can reduce the required amount of analyte (e.g., by employing microfluidic techniques), and second, one can reduce the amount of consumable per analyte volume which requires improved signal-to-noise discrimination.

In the following, we will discuss various approaches to resolve the drawbacks of conventional flow cytometers regarding their use for POC diagnostics.

3.1.2 Miniaturized Flow Cytometers and Microfluidic-Based Approaches

In recent years, a number of scaled-down "high-end" flow cytometer instruments and microfluidic-based devices for POC diagnostics have been developed with the promise of portability and reduced cost. The main driver for this development is the urgent need to perform CD4 T-lymphocyte counts in resource-limited settings. This is required for screening, initiation of treatment, and monitoring of HIV-infected patients [5].

Flow-based analysis with instruments such as the FACSCount™ (Becton Dickinson), EPICS XL/MCL™ (Beckman Coulter), Guava EasyCD4™ (Millipore/Merck), PointCare NOW™ (PointCare Technologies), or CyFlow CD4™ (Partec GmbH) is the established method for CD4 counting. However, these are still quite expensive and sophisticated instruments, requiring a lab environment and skilled operators. In addition to the established instruments, there are several under development or have recently entered the market that are especially designed for POC testing (e.g., from Axxin Ltd., Alere, Daktari Diagnostics, mBio Diagnostics, Partec and Zyomyx). These instruments are discussed in greater detail in a recent review article by Boyle et al. [6]. They are fast, quite robust, use a disposable cartridge, and need only a small amount of analyte (e.g., finger prick of whole blood). From this list, the recently introduced CyFlow miniPOC from Partec is the only instrument that represents a miniaturized flow cytometer, tailored to the needs of CD4 counting in the field. The others use different detection schemes to provide the cell count.

The CD4 test reader from Axxin measures the concentration of a cell-associated CD4 protein in whole blood rather than actually counting the CD4 cells. The PIMA™ instrument from Alere is based on cell capturing, microfluidic sample processing, and digital dual-color fluorescence image analysis. The device under development by Daktari Diagnostics uses specific cell capturing in a microfluidic cartridge functionalized with CD4 antibody. Differences in binding affinity and effective shear forces are used to differentiate between lymphocytes and monocytes. The CD4 count is determined by measuring the impedance change induced by the released ions after lysing the captured CD4 cells. The SnapCount™ instrument developed by mBio Diagnostics is based on immunostaining and cell capturing in combination with a two-color fluorescence imaging system. The instrument-free CD4 counting device developed by Zyomyx uses a sedimentation technique based on functionalized magnetic beads. The CD4 count can be determined by eye from a scale reading on the tubing.

Besides the commercial developments discussed above, there are many very promising concepts and technologies for POC diagnostics discussed in the literature.

In the following, we will focus on techniques suitable for on-the-flow analyte characterization. Concepts relying on specific cell capturing, for example, in functionalized microfluidic devices with automated electrical or imaging detection will not be addressed.

Over the past decade, many concepts have been developed to simplify and miniaturize on-the-flow analyte characterization by utilizing microfluidic channels that integrate fluidic handling (e.g., pumping, valves), on-chip sample preparation (e.g., mixing), particle manipulation (e.g., flow focusing, on-chip sorting), and miniaturized optics [7, 8].

Several recent review articles give an excellent overview of microfluidic flow cytometer technologies [9–11]. We will concentrate on their fluidic handling and how this is relevant for POC flow cytometers.

Conventional flow cytometers use sophisticated flow cells which allow for hydrodynamic flow focusing, in which large amounts of sheath flow are used to confine the analyte particles into a narrow stream. Flow focusing guarantees a constant speed for all particles and prevents sticking to the flow cell wall. A major goal driving the development of microfluidic flow cytometers is to reduce overall size of the instrument and the required amount of analyte and sheath fluid. Microfabrication techniques can be used to realize low-cost and miniaturized flow chips; however, in order to enable analyte focusing with little to no sheath fluid, new concepts have to be implemented. Due to the parabolic flow profile in microfluidic channels, it is essential to either confine the particle path in order to ensure uniform particle velocity or to implement detection schemes which can handle the large velocity distribution. Many concepts have been suggested to achieve analyte focusing to align the particles in microfluidic channel. They include inclusion of mechanical structures in flow channels [12, 13] and the use ultrasound effects [14], to confine and align the cell in microfluidic channel. A very interesting approach uses the inertia of the fluid acting on particles in shaped microchannels to enable precise cell positioning in the stream [15–19]. This technique allows for sheathless positioning and can be used to concentrate particles to a focused position. Moreover, it has been suggested that this approach also evenly spaces cells and particles along the direction of flow and potentially minimizes coincident detection [20]. Unfortunately, the inertial focusing depends on particle properties (e.g., size, shape), dimensions of the channel, and process parameters (e.g., particle speed). For instance, smaller particles need a longer distance to reach their stable positions in microfluidic channels. Consequently, this concept does not represent a general solution for sheathless analyte focusing in microfluidic-based flow cytometer. Even though designed and optimized for a specific application, this approach might be a very good solution. Using curved microfluidic channels combined with two-dimensional sheath flow provides a solution for particle focusing which is less elegant but also less critical [21]. The inclusion of chevron-shaped mechanical structures at the channel wall is another very interesting concept for hydrodynamic focusing in microfluidic channels [22]. The chevrons cause the sheath fluid provided from one or two sides to embed the analyte stream from all sides.

Microflow cytometers are being developed and tested in many labs for various applications, including blood analysis [23], CD4 counting [13], multiplexed bead assays [24], and ocean water monitoring [25,26]. A group at NRL has demonstrated simultaneous diagnosis of 12 different infectious diseases in serum [24] using bead-based assays and is currently integrating on-chip sample processing for POC use as a 30-min test. This group is also testing their microflow cytometer for real-time measurements of marine phytoplankton populations based on size and intrinsic fluorescence from chlorophyll and other light-harvesting pigments [25, 26]. This group claims that unlike most other microflow cytometers, their system can analyze cells ranging in size from 1 to over 100 μm. Researchers at Los Alamos National Laboratory have tested and evaluated very inexpensive lasers [27] and data systems [28]. Their goal is to reduce the cost of conventional flow cytometry and make them more widely available for point-of-care applications. A group at Purdue University is developing a LED-based microfluidic cytometer with integrated sample preparation. They have demonstrated the feasibility of using magnetic nanoparticles for on-chip sorting of human white blood cells from red blood cells and subsequent analysis of white blood cell subsets using antibody-labeled quantum dots [23]. This work as well as many other activities on this field is driven by the vision to develop an integrated handheld, portable, battery-powered unit for rapid blood analysis from a single drop of whole blood that is completely processed on-chip.

To date no flow cytometer meets all technical requirements for POC detection; in particular, the cost target remains extremely challenging. However, there are many interesting concepts under development. Especially the ones based on microfluidic flow cells look very promising. Based on the recent progress in this field, one can be cautiously optimistic that low-cost microcytometers for POC diagnostics will be available soon.

3.2 On-the-Flow Analyte Characterization Based on Spatial Modulation Technique

3.2.1 Spatially Modulated Fluorescence Emission: The Enabling Technique

PARC has demonstrated a new optical detection technique that delivers high signal-to-noise discrimination without precision optics to enable an optofluidic detector that can combine high performance, robustness, compactness, low cost, and ease of use. Detection sensitivity and analyte throughput can meet or even exceed the specifications of currently available (commercial) high-performance flow cytometers with the addition of point-of-need compatibility.

The enabling technique is termed “spatially modulated emission” and generates a time-dependent signal as a continuously fluorescing (bio-)particle traverses a

predefined pattern for optical transmission. Correlating the detected signal with the known pattern achieves high discrimination of the particle signal from background noise. In conventional flow cytometry, the size of the excitation area is restricted to approximately the size of the particle. With the spatial modulation technique, a large excitation area (ca. 0.1×1 mm) is used to increase the total flux of fluorescence light that originates from a particle. Despite the large excitation area, the mask pattern enables high spatial resolution which permits independent detection and characterization of near-coincident particles, with a separation (in the flow direction) that can approach the dimension of individual particles. In addition, the concept is intrinsically tolerant to background fluorescence originating from constituents in solution, the materials of the fluidic structures, or contaminants on surfaces.

To apply the spatially modulated fluorescence emission technique to particles moving through a fluid channel, a spatially patterned mask modulates the intensity of the fluorescent light incident on the photo detector over a large excitation area as illustrated in Fig. 3.1. The time dependence of the signal is defined by the spatial structure of the stripes of the mask and the speed of the particle. The recorded signal is analyzed by correlation techniques, and the intensity and time when the particle traverses the detection zone are accurately calculated. With state-of-the-art real-time correlation techniques, characterization for particle speeds up to a few meters per second is possible. The correlation analysis not only allows for very sensitive and reliable particle detection, but it also reveals the speed of each particle (see Fig. 3.1) which ultimately enables simple fluidic handling and true volumetric determination of the analyte. The basic concept, its lab implementation, and first proof-of-concept demonstration are described in [29]. The correlation analysis is described below in Sect. 3.2.2, and applications of the spatial modulation technique for detection bioparticles are presented in Sects. 3.2.3, 3.3, and 3.4.

3.2.2 Data Evaluation and Correlation Analysis

The data analysis relies on the concept of a matched filter. A matched filter correlates a known model signal, or template, with the stream of sensor data in order to detect the presence of the model signal within the stream. The mathematical operation computes the dot product of the template, $T = (T_1, T_2, \ldots, T_n)$, with the time series, $t_1, t_2, \ldots$, at each possible position j, that is, we compute $D_j = \sum_i T_i.t_{j+i}$, for each choice of j, and then declare a detection whenever D_j exceeds some threshold chosen to balance the two types of errors, false positives and false negatives. The template may be a theoretical pattern or, as shown in Fig. 3.2, derived from previously detected signals. As a speedup, we can compute D_j for many choices of j at once using the fast Fourier transform (FFT) to compute a convolution, rather than separately computing D_j for each choice of j. The matched filter technique, which dates back to World War II applications in radar and sonar, is a mathematically optimal detector for well-separated signals with additive white Gaussian noise. The technique can detect signals at remarkably low signal-to-noise

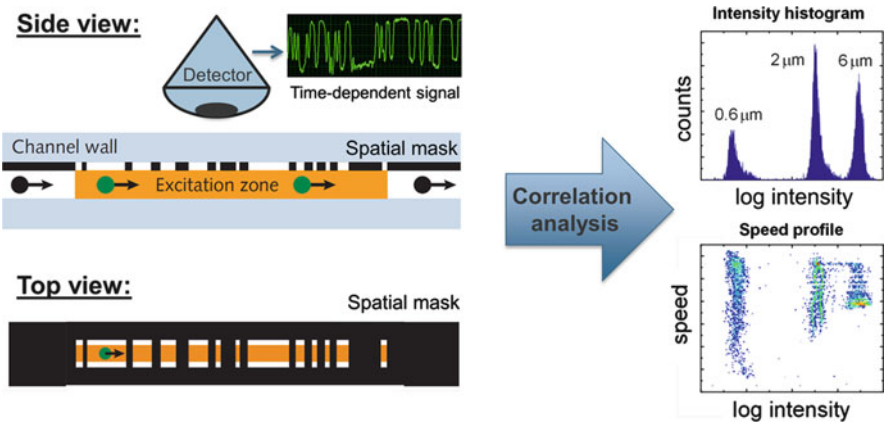

Fig. 3.1 Schematics illustrating the concept of spatially modulated emission. (*Left*) A patterned mask modulates the fluorescent light emitted from a particle flowing through a μ-fluidic channel directed to a large-area detector. Correlation analysis compares the measured signal and expected particle signatures. (*Right*) Data evaluation results in an intensity histogram and a speed profile of the detected particles that allows extraction of particle count and analyte volume, respectively

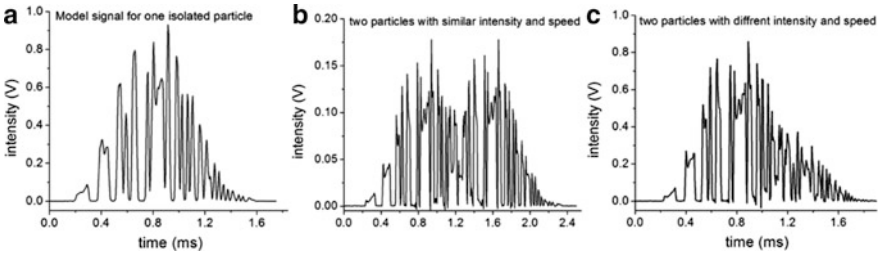

Fig. 3.2 Time-resolved signals with spatial modulation: (a) high SNR particles serve as templates for the expected mask pattern. An improved model signal can be generated by aligning and averaging multiple observed signals. (b) Overlapping signals from calibration beads with similar SNR. (c) Overlapping signals from calibration beads with different SNR. The second particle is approximately a factor of four weaker in intensity and 30% faster than the first one

ratios (SNR), often picking out a signal that cannot be detected by eye from a plot of the time series. Complicating the situation, however, are several factors: nonwhite noise, varying speeds of particles, overlapping signals, multiply tagged particles, and multiplexed masks.

3.2.2.1 Nonwhite Noise

If the noise in the sensor and electronics really were additive white Gaussian noise, spatial modulation would offer no sensitivity advantage, because a mask with no pattern on it would give a one-pulse signal just as detectable as a periodic signal from a striped mask. White noise, however, is a mathematical abstraction, and the

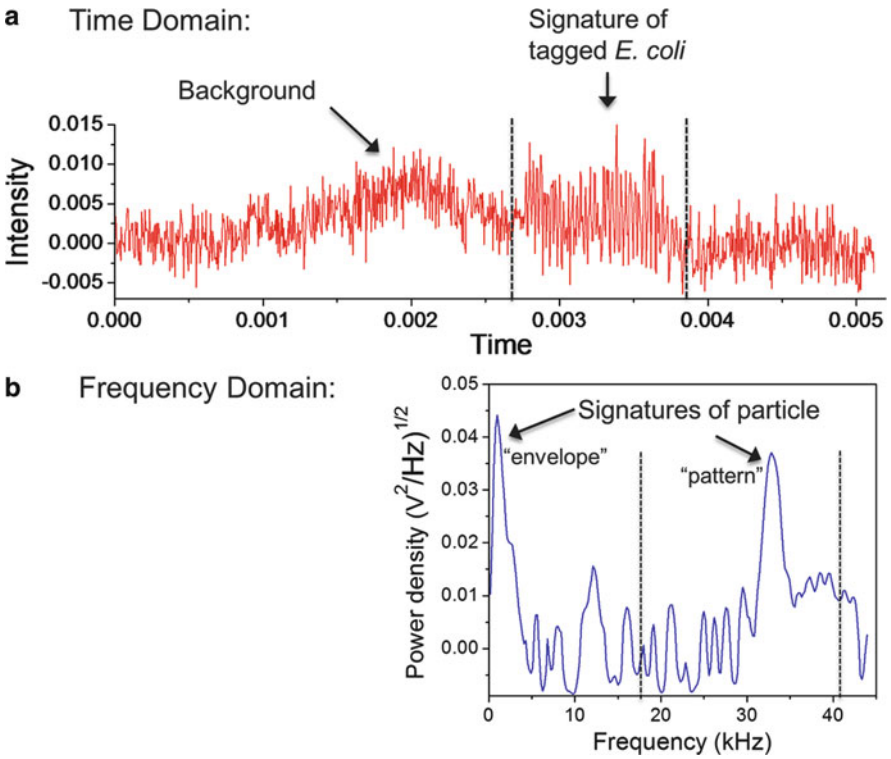

Fig. 3.3 Analysis of spatial modulation signal: (a) the time series above shows 5 ms of fluorescence intensity data. A particle is passing by the mask and its fluorescence signal is detected. While the absolute fluorescence intensity is not higher than the background, a clear pattern can be discerned. Therefore a typical threshold algorithm would fail to detect this particle. (b) Smoothened FFT of Figure 3.3a: The periodic signal from a particle passing a striped mask appears between 17 kHz and 40 kHz, depending upon the speed of the particle. Thus even a signal with low SNR still results in a strong peak in the frequency domain. Additionally an envelope peak for the detection duration of the particle occurs at a lower frequency. In Figure 3.3a, a particle is detected for approximately 1 ms, resulting in an envelope peak at 1 kHz in the FFT spectrum

noise from the sensor and electronics (Fig. 3.3) actually has power level decreasing quite markedly with frequency. In this case, spatial modulation offers a great advantage: by varying the width of the stripes in the mask, we can place the signal in a higher frequency region and thereby improve the effective SNR by 10× or more. The advantage is greatest for periodic signals of known frequency and long duration.

3.2.2.2 Varying Speeds of Particles

Our simple, low-cost, compact flow cytometer design moves complexity from hardware to software by allowing the speed of particles to vary within the channel and compensating for this variability computationally. The software computes the

correlation of the time series with many different templates, each a resampled version of a master template with a different sample rate. The software declares a detection if any dot product exceeds a settable threshold. There is one subtlety: faster particles give smaller dot products, so for accurate measurement of fluorescence intensity, templates must be scaled to correct for this (not-quite-linear) effect. With coded masks, and hence aperiodic signals, there may also be an issue with computational speed. Simultaneous correlation with a great many templates may be slow, even with FFTs, so we generally use templates at fairly coarse steps, for example, 1 m per second, 1.02, 1.02^2, 1.02^3, and so forth. Dependent upon the channel geometry and particle sizes, speed can vary by 3× from slowest to fastest, so that up to ∼60 templates may be necessary.

With a regularly striped mask and periodic signals, there is no need to compute the correlation with many different templates. In this case, the signal is sufficiently concentrated in the frequency domain that a simple algorithm suffices (Fig. 3.2), one that declares a detection if any single power spectrum value within the expected frequency range exceeds background values by a preset threshold. We have found, however, that this simple algorithm is best used only to detect the presence and approximate speed of a particle, with accurate intensity computed using time-domain correlation as before.

3.2.2.3 Overlapping Signals

With a large-area sensor, there is a significant chance of sensing two or more particles at once. Overlapping signals (Fig. 3.2) can be hard to detect and separate, especially in the case of periodic signals and unequal intensities. The data analysis software takes a two-pass approach: it detects isolated particles first, removes them, and then detects what is left of overlapping particles. This approach appears successful for particles that overlap by less than ∼80 %, at which point even the human eye cannot reliably separate the signals. Except in the case of particles that physically stick to each other, we have found that overlapping signals occur at the rate one would predict by a Poisson process, that is, if there is at least one particle in the detector 20 % of the time, then there are two particles about $0.2 \times 0.2 = 4$ % of the time. Aperiodic masks are more reliable than periodic masks for the detection of overlapping particles because two particles of the same speed but opposite phase can sum to a long blur rather than a periodic signal as they pass behind a periodic mask. Not all aperiodic masks are equally good at separating overlapping particles, and mask designs that give low autocorrelation side lobes (e.g., masks based on Barker codes) outperform other masks.

3.2.2.4 Multiply Tagged Particles

As described below, we have run particles tagged with two dyes, an identifier and a reporter, through a detector equipped with a periodic mask and two read-out

channels. The identifier channel has high SNR, so we can use the identifier channel to produce the template for correlation with the reporter channel. That is, the software detects particles by looking for a strong peak in the power spectrum of the identifier channel and then correlates the detected time-domain signal from the identifier channel, normalized for total intensity, with the reporter channel to measure reporter intensity. There is no need to compute the full convolution because the two channels are exactly synchronized.

3.2.2.5 Multiplexed Mask

Also as described below, we have also measured two differently tagged types of particles with a single read-out channel, by using a multiplexed mask modulated at one spatial frequency for one color and at another spatial frequency for another color. The two frequencies are at a known ratio of r. For this case, the algorithm detects particles by looking for a strong peak in the power spectrum and then classifies the particle by checking the power levels of frequencies r and 1/r times the detected peak. This algorithm gave error rate about 1 %, with the few errors resulting from overlapping signals.

3.2.3 CD4 Count in Whole Blood

The spatial modulation technique has been extensively evaluated with measurements of absolute CD4+ and percentage CD4 counts in human blood, which are required for screening, initiation of treatment, and monitoring of HIV-infected patients. And the technique has been benchmarked against a commercial instrument (BD FACSCount) with a direct one-to-one comparison of measurements on the same labeled blood samples, with excellent agreement for both absolute CD4 and CD4% as discussed in [30].

The evaluation was performed with a prototype bench-top instrument capable of measuring absolute CD4, CD8, and percentage CD4 in whole blood. A sample of tagged blood could be analyzed in less than 5 min. Sample preparation required only simple dilution, mixing, and incubation steps, with no lysing or washing step. The mixing was performed by repeatedly pipetting the sample-analyte mixture into a vial.

Measurements of CD4 were conducted on samples of whole blood. The samples were prepared with the standard BD CD4 reagent (PE-CD4, PE/CY5-CD3, and known number of fluorescent microbeads) and a recently introduced FACSCount CD4% reagent kit (BD#339010) that consists of a single tube containing a mixture of the following: three monoclonal antibodies CD4/CD14/CD15 (conjugated with PE/PE-Cy5/PE-Cy5, respectively), a nucleic acid dye, and a known number of fluorescent microbeads. The antibody to CD14 recognizes a human monocyte/macrophage antigen, whereas the antibody to CD15 recognizes

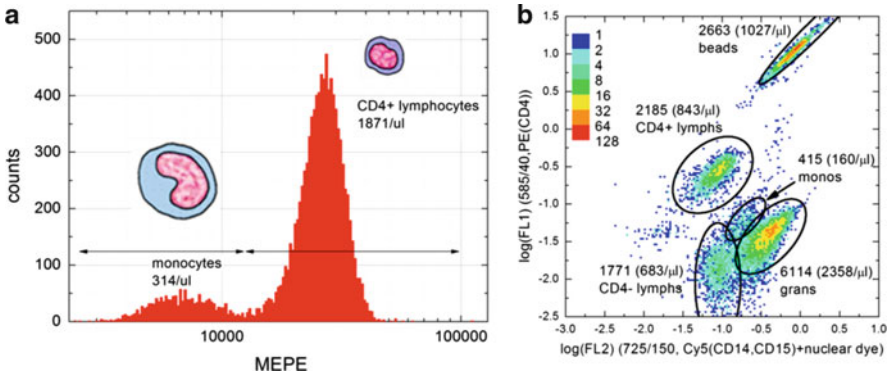

Fig. 3.4 (**a**) Histograms of detected CD4 cells in whole blood (dilution 5:1) as a function of fluorescent intensity. This illustrates an absolute CD4 count in whole blood (no lyse, no wash, dye: PE) (Adapted from [30]). (**b**) CD4% measurement obtained from whole blood (no lysing) with PARC's spatial modulation technique. The pattern agrees in all essential features with that from a commercial BD FACSCount instrument (Adapted from [30])

a human myelomonocytic antigen that is present on the majority of granulocytes. No lysing of the red blood cells or washing steps to separate the tagged blood cells from unbound dye were used. We have tested a variety of blood samples with different dilutions (1:10 to 1:1 blood to buffer ratio), incubation times (10–40 min), and temperatures (RT, 37° C).

A histogram of detected CD4 cells in whole blood (no lyse, no wash, dye: PE) is shown in Fig. 3.4a as a function of fluorescent intensity. Sample preparation was as follows: 25 µl whole blood, 2 µl CD4-PE, and 123 µl PBS, dilution of 1:5. This illustrates a CD4 count in whole blood (no lyse, no wash, dye: PE). The plots exhibit two peaks that are attributed to CD4 lymphocytes (right peak) and CD4 monocytes (left peak). This histogram is representative for many measurements on this donor blood (i.e., for repeated measurements on the same sample and samples with modified sample preparation). The average absolute CD4 count was ~1,800 CD4 cells per µl blood with a variation of about ±6 %. The recorded CD4 count is at the upper end but within the expected range for human blood. The relative count rate of lymphocytes and monocytes and, more importantly, the peak distance (intensity ratio) are in good agreement with data reported in the literature [31].

Measurements of %CD4 were conducted on samples of whole blood that were stained with BD CD4% reagent (BD#339010). For this measurement, two fluorescence signals were simultaneously recorded from the same detection area. They were recorded from opposite sides of the fluidic chip. A volume of 30 µl of analyte containing 3 µl of whole blood (specified protocol for the CD4% reagent) was analyzed within 5 min. The sample was prepared by following the recommended BD sample preparation protocol to obtain samples with a dilution of 1:10.

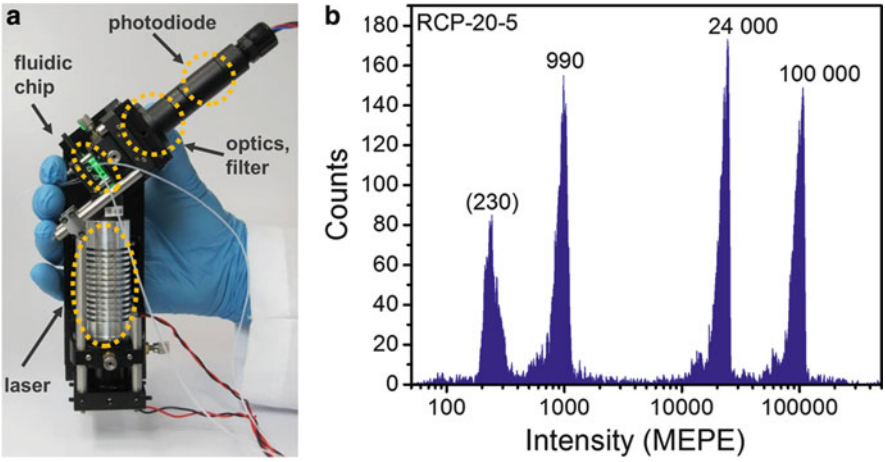

Fig. 3.5 *Left*: Prototype of a compact, low-cost, battery-powered, handheld flow cytometer. We used off-the-shelf components to assemble the ~5 × 3 × 2-in. instrument which weighs less than 1 lb. A battery pack of similar weight is sufficient for more than 10 h of continuous operation. *Right*: Intensity histogram of a sample of 2 μm Rainbow calibration beads (RCP20-5)

A representative density plot is shown in Fig. 3.4b with patterns for the major constituents of white blood cells (WBC). For comparison and benchmarking, measurements were performed on the same samples with a FACSCount (BD Biosciences). The patterns from the two instruments were in good agreement as discussed in [30].

Measurements of absolute CD4 were also successfully performed on samples with much higher blood concentrations of up to 1:2. The ability to analyze a large amount of whole blood per unit time enables either reduced analysis time or improved data statistics.

3.2.4 Handheld Prototype

The first generation of a compact, single-parameter optofluidic detector based on the spatial modulation technique is shown in Fig. 3.5. Its size is ~5 × 3 × 2 in., and we anticipate that the dimensions will shrink further in the final, engineered layout that will include laser diodes for excitation. For detection, we use a small high numerical aperture aspheric lens (NA 0.6, 6.3-mm diameter) and a basic pin photodiode rather than a photomultiplier tube (PMT). The prototype was assembled with off-the-shelf components (~$350, excluding pumps and housing), and the optical unit can be battery powered (2 × 9 V, 4 × 1.5 V AA-type are sufficient for >10 h continuous operation).

The prototype uses sheath flow from two sides of the 25 μm-high and 120 μm-wide fluidic channel. This channel is part of a custom fluidic chip that has the spatial shadow mask directly attached to it and that also serves as a light guide for the excitation laser.

Measurements of the sensitivity and dynamic range of the prototype were conducted with 2 μm Rainbow calibration beads (Spherotech) and yielded a detection limit ~200 MEPE (molecules of equivalent phycoerythrin) [32], which meets the needs for a wide range of bioparticle detection applications. By replacing the pin photodiode by a pixelated avalanche photodiode, the sensitivity increases to 50 MEPE which meets or even exceeds the specifications of current commercial high-performance flow cytometers.

3.3 Pathogen Detection in Water

3.3.1 Background and Currently Used Techniques

Water-quality monitoring is an essential priority for global health. The United States Environmental Protection Agency (EPA) and Centers for Disease Control and Prevention (CDC) estimate that there are 4–12 million cases of acute gastrointestinal illness annually attributable to public drinking water systems in the USA [33]. With microorganisms a primary cause for the occurrence of infectious diseases, the concentrations of harmful microbes should be routinely monitored to maintain microbiological quality control of drinking water.

Because of the difficulty and cost of directly measuring all microbial pathogens in water samples, organisms like coliform bacteria, *Giardia,* and *Cryptosporidium* that indicate the presence of sewage and fecal contamination have been targeted for measurement [34]. There is a strong need for an inexpensive, rugged, and fast detection instrument to monitor both beaches and drinking water at the point of need.

Bacterial quantification is currently performed by labs primarily using plate culture assay techniques that have supported microbiology for more than 100 years. The gold standard to determine bacterial coliform count in water starts with the membrane filter technique, then incubation growth in a plate culture followed by counting of the colony-forming units. Unfortunately, culture assay techniques for quantification are costly, labor intensive, and time-consuming to conduct with measurement times greater than 24 h due to incubation needs. Culture-independent techniques have used fluorescent microscopes, but the method is labor intensive and differences in the numbers of bacteria observed can arise due to staining technique, physicochemical characteristics of the samples, and investigator bias [35]. A method using TaqMan PCR has been developed to quantify indicator bacteria rapidly [34], but the instrument is bulky and expensive so the sample is still sent to the lab for analysis with the samples usually kept on ice during the time before analysis.

Flow cytometry as an effective and well-established method for counting cells on a large scale is also used to detect microorganisms in water [36]. Flow cytometers allow sensitive and reliable quantification of individual cells; however, as noted earlier, this technique requires expensive equipment and is skill- and labor intensive. Microfluidic devices have the potential to increase ease of use by integrating sample pretreatment and separation strategies. Recently, flow cytometer research with microfluidic devices has shown detection and quantification of bacteria [37,38], by using fluorescently labeled anti-*E. coli* antibodies to selectively detect *E. coli*. Flow cytometry has also been used to detect quantitatively *Giardia* cysts and *Cryptosporidium* oocysts [39–41]. These studies evaluated the staining efficiencies for commercial antibodies and suggest that flow cytometry is a precise method for the detection of *Giardia* and *Cryptosporidium* in water. Antibodies for immunofluorescence staining are available for most of the targeted waterborne pathogens.

The monitoring of drinking water is currently mostly performed by filtering and culturing techniques and represents a substantial part of workload of microbiology laboratories [42]. Waterborne bacterial pathogens and indicators are often physiologically altered/stressed and sometimes cannot be cultured efficiently with standard techniques [43]. This can lead to a considerable underestimation of the concentration of these bacteria in water and therefore of their risks to human health. In contrast, flow cytometry can detect bacteria in all stages. With appropriate staining (e.g., propidium iodide (PI)), flow cytometers can be used to distinguish between viable and nonviable cells [44].

3.3.2 Pathogen Detection in Water with Spatially Modulated Emission

Our prototype instrument can also be used to reliably identify and count specifically tagged pathogens (e.g., *E. coli*, *Giardia,* and *Cryptosporidium*) in water. For example, Fig. 3.6a shows the intensity histogram and the speed profile for *Giardia lamblia* stained with an anti-*Giardia* monoclonal antibody conjugated with Cy3. Incubation studies were performed to determine the required staining time and amount of reagent. As shown in Fig. 3.6b for *G. lamblia*, a reagent-to-analyte volumetric ratio of 1:100 and an incubation time of less than 2 min are sufficient for reliable detection. Note that even for this data point the pathogen signal ($\sim 10^5$ MEPE) is more than two orders of magnitude separated from the noise. A one-step staining method consisted of addition of the fluorescently tagged antibody to the *G. lamblia* sample, mixing, and incubation steps. No additional steps, such as washing to remove unbound antibody, were necessary prior to measurement. The results from the incubation study indicate that this particular application is compatible with rapid on-chip sample preparation.

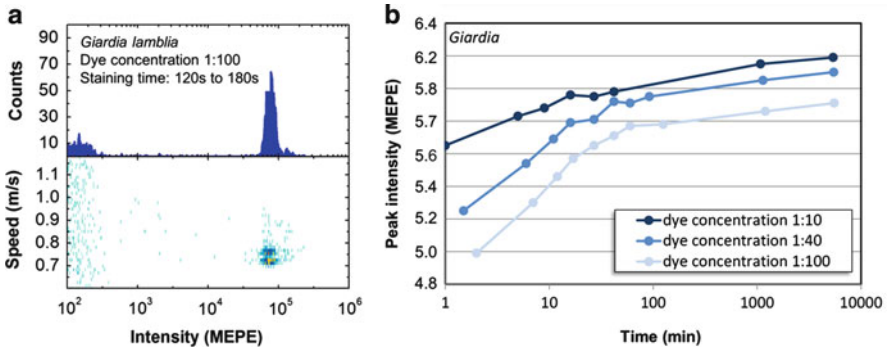

Fig. 3.6 *Left:* Intensity histogram and speed profile for *Giardia lamblia* cysts measured with prototype instrument shown in fig. 3.5 *Right:* Incubation study for *Giardia lamblia.* Our experiments showed that even for an analyte/reagent ratio of 100:1 a staining time of $\sim$ 2 min is sufficient for reliable detection. We used a very simple sample preparation: mixing, incubation, no wash. On-chip sample prep seems straight forward for this test

3.4 Multiplexed Flow Assay

For advanced diagnostics, multiple biomarkers within a complex biological sample need to be simultaneously detected and quantified (proteins, cells, DNA fragments, (bio)molecules, etc.). For quantification of cellular markers, for example, CD4 cells, flow cytometry is an obvious choice. The size of cells is well compatible with the flow cytometer technology. Thousands of staining assays provide the sensitivity and specificity for intra- and cell surface markers that can be detected, enumerated, and quantified in flow cytometers. The detection of smaller individual bioparticles, for example, viruses, is less common [45] because fewer specific stains are available, fluorescent brightness and scatter signals are generally lower, and the small size of objects leads to inaccurate detection when multiple particles are present in the detection area. Especially the latter failure mechanism prevents specific direct quantification of biomolecules (e.g., proteins, DNA fragments) in solution.

In order to detect and quantify incorporated dyes of (bio-)molecules simultaneously, various detection schemes have been developed – enzyme-linked immunosorbent assay (ELISA) [46,47], DNA microchip [48,49], multiplexed SPR [50,51], etc.

The common characteristic of these techniques is the fact that different detection reagents are spaced in close proximity and the detection scheme takes position-resolved measurements. Different positions therefore identify different analytes. For any of these techniques, the detection positions are located on a surface, making the lateral diffusion lengths and times of analytes the relevant ones for the measurement.

For flow cytometer applications, multiplexed (fluorescent) particle-based assay have been developed and commercialized. These assays consist of different types of beads which can be distinguished by size (e.g., Assay Designs), emission

intensity of incorporated dyes (e.g., BD™ Cytometric Bead Array), or color of incorporated dyes (e.g., Luminex). In the assays that use particles filled with fluorescent dyes, different dye concentrations are used to label different classes of beads, while size-encoded classes of beads are measured with scatter signals. The dye intensity/color and thereby the class of particle are determined in one or more fluorescence excitation/emission channels, while the quantification of the target molecules is performed in an additional fluorescence channel. Beads of one class are functionalized with a specific primary antibody. Such a bead "collects" antigens (e.g., proteins) from the solution and binds them. After incubation and washing, a fluorescently labeled secondary antibody is added. This antibody binds specifically to all target proteins. The amount of secondary antibody bound to the bead is a measure for the concentration of the target molecule in the sample; it is detected by the fluorescence intensity of the secondary antibody's label. This means that the identifying fluorescence of the particle (class) provides a trigger and the specificity of the system, while the fluorescence of the secondary antibody quantifies the target analyte concentration – it provides the sensitivity. The concept of using two antibodies is often referred to as "sandwich assay," and it is also commonly used in ELISA. Therefore, bead-based analyte identification and quantification is frequently called "ELISA on the flow."

Such multiplexed assays have been developed and commercialized, for example, for human cytokine profiling [52, 53]. In order to provide additional flexibility in microfluidic sample preparation, magnetic beads that carry fluorescent identifiers have also been developed and are commercially available [54].

A prominent example for a color-coded multiplexed bead assay is the Luminex xMap technology [55] which provides up to 100 classes by using concentration combinations of two dyes. These dyes can be excited at 635 nm, and their emission maxima are around 660 and 710 nm. PE-fluorescence – excitable at 532 nm with an emission maximum at 575 nm – is used for the quantification of the secondary antibody. Therefore, the three fluorescent labels sufficiently differ in their excitation/emission spectra to ensure a correct identification of the beads without cross talk from the identifying dyes into the quantifying channel.

We have demonstrated that our microfluidic detection platform is capable of analyzing multiplexed flow assays. We have set up an instrument with two lasers (532 and 635 nm) and three fluorescence channels. Fluorescence light was collected and filtered with a 535-nm-long pass filter. Subsequently, the detected light was sent through a 648-nm dichroic mirror. The reflected portion of the light was sent through a 585/40-nm band-pass filter onto the quantifier channel detector. Light that was transmitted through the first dichroic mirror was directed through a 635-nm-long pass filter to a second dichroic mirror (685 nm). This mirror splits the classifying dye emission to two additional detectors, one filtered with a 660/32 nm and the other filtered with a 716/40-nm band-pass filter.

Luminex xMap beads were identified, and thyroid-stimulating hormone concentrations were detected down to 0.1 μIU/ml in this setup. Figure 3.7 shows results for Luminex calibration beads for testing the identifier (CON1) and reporter (CON2)

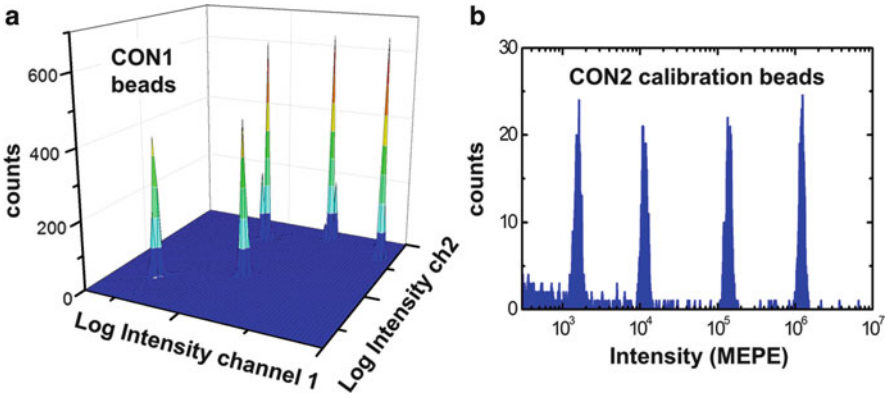

Fig. 3.7 Results for Luminex xMap bead. The results for the CON1 calibration beads (identifier channel) illustrate the ability to distinguish between different bead types, and the results for CON2 show the ability to detect low analyte concentrations (reporter channel)

channel. This measurement illustrates that we can clearly distinguish the different bead types and that we have a sufficient sensitivity in the reporter channel to measure low analyte concentrations.

3.5 Multicolor Detection with Single Large-Area Detector

The particular strength of our technique is to enable sensitive, rugged, and low-cost instruments for PoC applications. The critical alignment within the system is substituted by the alignment of the shadow mask relative to the channel thereby providing a rugged system. To prove multicolor detection can be achieved without costly dielectric filter sets and multiple detectors, we demonstrated an elegant and effective solution for two-color detection using a single larger-area detector. Replacing the patterned shadow mask with a patterned color mask (see Fig. 3.8a) allows recording multiple fluorescence channels with a single large-area detector. Different fluorescence emission characteristics of different fluorophores are transmitted at different positions of the mask. Therefore, different fluorophores create a different fluorescence intensity-time profile when they traverse the detection area. Information of the particle's emission spectrum is encoded in the time-dependent signal.

In our measurements, we used a 532-nm excitation laser, a pin photodiode, and a red/green-patterned color mask to distinguish between PE and PECy5 Spherotech beads. PE-fluorescence emission is transmitted by the green parts of the transmission mask shown in Fig. 3.8a, while PECy5-fluorescence emission is transmitted by the complementary red parts of the mask. As shown in Fig. 3.8b, the fluorescence signal from PE and PECy5 Spherotech beads which have the same excitation spectra but different emission spectra shows a (almost) complementary

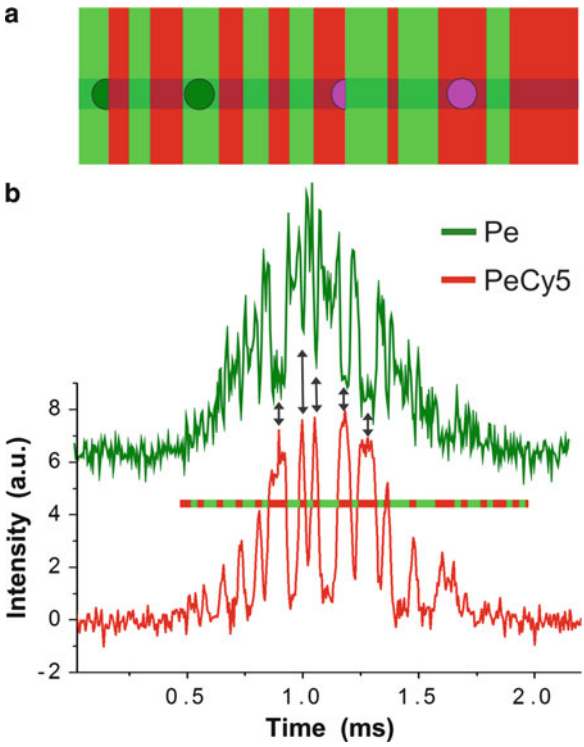

Fig. 3.8 Multicolor detection: (a) schematics of the transmission characteristics of a patterned color mask. Light from "green" particles are only visible through the green area of the mask. (b) PE and PECy5 Spherotec Beads excited at 532 nm and detected with a red/green patterned color mask. The transmission maxima of the PE bead coincide with transmission minima of the PECy5 Bead. With the color mask spectral information are converted into time variation of the detected intensity as indicated in Fig 3.8b by the overlaid mask pattern

fluorescence intensity-time pattern. Therefore, they can be identified based on their emission characteristics in a new way, that is, one that does not need multiple detectors, multiple filters, or dichroic mirrors.

We have also tested this characterization method by using the superposition of two periodic red and green masks with corresponding 33 and 23 transmission periods. PE and PECy5 beads showed clearly distinguishable time patterns in this setup. In particular, the fast Fourier transformation of the signal showed different ratios for the contribution of the fast emission frequency (resulting from the red parts of the mask) and the slow emission frequency (resulting from the green parts of the mask) for different beads. Based on this information, we characterized beads automatically while simultaneously determining their fluorescence intensity and their speed.

3.6 Summary and Outlook

The majority of biological and biomedical tests are performed at major, centralized clinical laboratories because the availability of compact, robust, and inexpensive instruments for POC testing is very limited. Yet there are compelling factors driving

the development of POC testing that include reduced costs, timely test results, lower mortality rates, and reduced morbidity.

Today's flow cytometers are sophisticated analytical instruments that are extensively used in research and clinical laboratories. Their complex measurement principles make it challenging to package such a system into a mechanically rugged, compact, low-power, and inexpensive instrument. However, for the clearly defined use of CD4 and CD4% testing, such an instrument is now commercially available (Partec, CyFlow miniPOC), and we are certain that similar devices for other applications will follow. The applicability of a flow cytometer in the field will be evaluated, and this device and others will be continuously improved based on field experiences.

In particular, the cost of devices and the cost per test will be a driver for further development for any POC testing device. Smaller sizes, more functionality, better accuracy, etc., will be naturally included in the next generation of these devices. Blood glucose meters for diabetics are probably the best example for this development outline. Today, however, no POC flow cytometer has a maturity that is comparable to any given blood glucose meter.

The technical challenges for a POC flow cytometer can be grouped into two sets of problems – fluidic handling and optical detection.

Most advanced POC devices will require sample preparation steps. Sample preparation represents a major source of errors, in particular if performed by minimally trained operators. Skilled operators on the other hand are a significant cost factor in testing, but they still do not guarantee error-free operation. Therefore, automatic sample acquisition and preparation of minimal amounts is a benefit for any biomedical POC (or conventional) testing device. Numerous microfluidic and fluidic chip-based sample handling approaches have been presented and implemented: on-chip cell lysing, microfluidic separation of white blood cells, and automated specific staining of cells only to name a few.

The basis for on-chip sample preparation is in most cases reliable fluidic handling. This includes actuating, valving, mixing, and metering nano- to microliters of various liquids. To avoid large external pumps, the need for pressure lines, and complex pressure interfacing with a fluidic chip, which would contradict the idea of a portable POC devices, on-chip fluid handling has been developed. An impressive toolbox of fluid handling techniques has been developed, many different complete fluidic solutions have been demonstrated, and the field is still rapidly progressing.

At PARC, we have mainly focused on demonstrating and benchmarking a new optical detection technique that meets the requirements of POC devices. "Spatially modulated fluorescence emission" delivers high signal-to-noise discrimination without precision optics to enable robustness, compactness, and low cost in POC flow cytometers. The design is based on a large-area optical encoding-decoding mechanism rather than a redesign of a classical flow cytometer.

Our detection technique generates a time-dependent signal as a continuously fluorescing bioparticle traverses a predefined pattern for optical transmission. Correlating the detected signal with the known pattern achieves high discrimination of the particle signal from background noise.

Our method is intended to overfill a large excitation area to increase the total flux of fluorescence light that originates from a particle and to be relatively alignment insensitive. The large excitation area could be illuminated by an LED rather than a laser, a feature that cannot be achieved in classical flow cytometer setups. The mask pattern enables a high spatial resolution – comparable to classical flow cytometers – and it is aligned relative to the flow channel during the production of the fluidic chip.

The detection technique has been extensively evaluated with measurements of absolute CD4+ and percentage CD4 counts in human blood. More recent experiments demonstrate that the platform can address a large variety of diagnostic needs including multiplexed bead-based assays and identification and enumeration of pathogens (e.g., *Giardia*, *Cryptosporidium,* and *E. Coli*) in fluids.

We foresee that the future of most POC testing devices lies in the integration of sample collection and preparation into a disposable cartridge. We have described an optical detection technique that is compatible to this approach because it provides the necessary alignment tolerance, sensitivity, and price reduction.

Acknowledgment The work on the spatial modulation technique and its application in flow cytometry was partially supported by grants from the National Institute of Health (5R21EB011662-02) and the US Army Research Office (W911NF-10-1-0479).

References

1. J. Carey, J. McCoy, D. Keren, (eds.), *Flow Cytometry in Clinical Diagnosis.*, 4th edn. (American Society for Clinical Pathology, Singapore, 2007).
2. H.M. Shapiro, *Practical Flow Cytometry* (Wiley, Hoboken, 2005).
3. M. Rieseberg, C. Kasper, K.F. Reardon and T. Scheper, Flow cytometry in biotechnology. *Appl. Microbiol. Biotechnol.* **56**(3–4), 350–360 (2001).
4. R.A. Hoffman, Flow cytometry: instrumentation, applications, future trends and limitations, in *Standardization and Quality Assurance in Fluorescence Measurements II*, ed. by U. Resch-Genger (Springer, Berlin/Heidelberg, 2008)
5. WHO, Antiretroviral therapy for HIV infection in adults and adolescents. Recommendations for a Public Health Approach (2006). http://www.who.int/hiv/pub/guidelines/artadultguidelines.pdf
6. D.S. Boyle, K.R. Hawkins, M.S. Steele, M. Singhal and X. Cheng, Emerging technologies for point-of-care CD4 T-lymphocyte counting, Trends Biotechnol. **30**(1), 45–54 (2011).
7. X. Mao, J.R. Waldeisen, B.K. Juluri and T.J. Huang, Hydrodynamically tunable optofluidic cylindrical microlens. Lab Chip **7**(10), 1303–1308 (2007).
8. X. Mao, S.C. Lin, M.I. Lapsley, J. Shi, B.K. Juluri, T.J. Huang, Tunable Liquid Gradient Refractive Index (L-GRIN) lens with two degrees of freedom, Lab Chip **9**(14), 2050–2058 (2009).
9. J.S. Kim, F.S. Ligler (eds.), *The Microflow Cytometer* (Pan Stanford Publishing, Singapore, 2010).
10. D.A. Ateya, J.S. Erickson, P.B. Howell, Jr., L.R. Hilliard, J.P. Golden, F.S. Ligler, The good, the bad, and the tiny: a review of microflow cytometry, Anal Bioanal.Chem **391**(5), 1485–1498 (2008).
11. J. Godin, C.H. Chen, S.H. Cho, W. Qiao, F. Tsai, Y.H. Lo, Microfluidics and photonics for Bio-System-on-a-Chip: a review of advancements in technology towards a microfluidic flow cytometry chip. J Biophotonics. **1**(5), 355–376 (2008).

12. A.L. Thangawng, J.S. Kim, J.P. Golden, G.P. Anderson, K.L. Robertson, V. Low, F.S. Ligler, A hard microflow cytometer using groove-generated sheath flow for multiplexed bead and cell assays, Anal Bioanal. Chem **398**(5), 1871–1881 (2010).
13. H. Yun, H. Bang, J. Min, C. Chung, J.K. Chang, D.C. Han, Simultaneous counting of two subsets of leukocytes using fluorescent silica nanoparticles in a sheathless microchip flow cytometer, Lab Chip **10**(23), 3243–3254 (2010).
14. G.R. Goddard, C.K. Sanders, J.C. Martin, G. Kaduchak and S.W. Graves, Analytical performance of an ultrasonic particle focusing flow cytometer, Anal. Chem. **79**(22), 8740–8746 (2007).
15. C.D. Di Carlo, J.F. Edd, K.J. Humphry, H.A. Stone M. Toner, Particle segregation and dynamics in confined flows. Phys. Rev. Lett. **102**(9), 094503 (2009).
16. S.C. Hur, H.T. Tse, D. Di Carlo, Sheathless inertial cell ordering for extreme throughput flow cytometry. Lab Chip **10**(3), 274–280 (2010).
17. C.D. Di Carlo, Inertial microfluidics. Lab Chip **9**(21), 3038–3046 (2009).
18. A.A. Bhagat, S.S. Kuntaegowdanahalli, N. Kaval, C.J. Seliskar I. Papautsky, Inertial microfluidics for sheath-less high-throughput flow cytometry. Biomed. Microdevices. **12**(2), 187–195 (2010).
19. J. Oakey, R.W. Applegate, Jr., E. Arellano, C.D. Di Carlo, S.W. Graves, M. Toner, Particle focusing in staged inertial microfluidic devices for flow cytometry. Anal. Chem. **82**(9), 3862–3867 (2010).
20. W. Lee, H. Amini, H.A. Stone C.D. Di Carlo, Dynamic self-assembly and control of microfluidic particle crystals. Proc. Natl. Acad. Sci. U. S. A. **107**(52), 22413–22418 (2010).
21. X. Mao, S.C. Lin, C. Dong T.J. Huang, Single-layer planar on-chip flow cytometer using microfluidic drifting based three-dimensional (3D) hydrodynamic focusing. Lab Chip **9**(11), 1583–1589 (2009).
22. P.B. Howell, Jr., J.P. Golden, L.R. Hilliard, J.S. Erickson, D.R. Mott, F.S. Ligler, Two simple and rugged designs for creating microfluidic sheath flow. Lab Chip **8**(7), 1097–1103 (2008).
23. M.M.G. Grafton, T. Maleki, M.D. Zordan, L.M. Reece, R. Byrnes, A. Jones, P. Todd, J.F. Leary, Microfluidic MEMS hand-held flow cytometer, *Proceedings of the SPIE*, vol. 7929(Microfluidics, BioMEMS, and Medical Microsystems IX), 79290C-79290C-10 (2011), Techshot, (USA)
24. J.S. Kim, F.S. Ligler, Utilization of microparticles in next-generation assays for microflow cytometers, Anal. Bioanal. Chem **398**(6), 2373–2382 (2010).
25. N. Hashemi, J.S. Erickson, J.P. Golden, K.M. Jackson, F.S. Ligler, Microflow Cytometer for optical analysis of phytoplankton. Biosens. Bioelectron. **26**(11), 4263–4269 (2011).
26. N. Hashemi, J.S. Erickson, J.P. Golden and F. S. Ligler, Optofluidic characterization of marine algae using a microflow cytometer. Biomicrofluidics **5**(3), 032009-032009-9 (2011).
27. R.C. Habbersett, M.A. Naivar, T.A. Woods, G.R. Goddard, S.W. Graves, Evaluation of a green laser pointer for flow cytometry. Cytometry A **71**(10), 809–817 (2007).
28. M.A. Naivar, M.E. Wilder, R.C. Habbersett, T.A. Woods, D.S. Sebba, J.P. Nolan, S.W. Graves, Development of small and inexpensive digital data acquisition systems using a microcontroller-based approach. Cytometry A **75**(12), 979–989 (2009).
29. P. Kiesel, M. Bassler, M. Beck and N. Johnson, Spatially modulated fluorescence emission from moving particles. Appl. Phys. Lett. **94**(4), 041107 (2009).
30. P. Kiesel, M. Beck and N. Johnson, Monitoring CD4 in whole blood with an opto-fluidic detector based on spatially modulated fluorescence emission. Cytometry A **79**(4), 317–324 (2011).
31. W. G´ohde, U. Cassens, L.G. Lehman, Y. Traoré, J.W. G´ohde, P. Perkes, C. Westerberg, B. Greve, Individual patient-Dependent influence of erythrocyte lysing procedures on flow-cytometric analysis of leukocyte subpopulations. Transfus. Med. Hemotherapy **30**(4), 165–170 (2003).
32. P. Kiesel, J. Martini, M. Beck, M. Huck, M.W. Bern, N.M. Johnson, 'Spatially modulated emission' advances point-of-care diagnostics, Laser Focus World **15**(10), 47–50 (2010)

33. J.M. Colford, Jr., S. Roy, M.J. Beach, A. Hightower, S.E. Shaw, T.J. Wade, A review of household drinking water intervention trials and an approach to the estimation of endemic waterborne gastroenteritis in the United States. J. Water Health **4** (Suppl 2), 71–88 (2006)
34. T.J. Wade, R.L. Calderon, E. Sams, M. Beach, K.P. Brenner, A.H. Williams, A.P. Dufour, Rapidly measured indicators of recreational water quality are predictive of swimming-associated gastrointestinal illness. Environ. Health Perspect. **114**(1), 24–28 (2006)
35. R.L. Kepner, Jr., J.R. Pratt, Use of fluorochromes for direct enumeration of total bacteria in environmental samples: past and present, Microbiol. Rev. **58**(4), 603–615 (1994).
36. J. Vives-Rego, P. Lebaron, C.G. Nebe-von, Current and future applications of flow cytometry in aquatic microbiology. FEMS Microbiol. Rev. **24**(4), 429–448 (2000).
37. L. Yang, L. Wu, S. Zhu, Y. Long, W. Hang, X. Yan, Rapid, absolute, and simultaneous quantification of specific pathogenic strain and total bacterial cells using an ultrasensitive dual-color flow cytometer. Anal. Chem. **82**(3), 1109–1116 (2010).
38. M.A. McClain, C.T. Culbertson, S.C. Jacobson, J.M. Ramsey, Flow cytometry of *Escherichia coli* on microfluidic devices. Anal. Chem. **73**(21), 5334–5338 (2001)
39. J. Barbosa, S. Costa-de-Oliveira, A.G. Rodrigues, C. Pina-Vaz, Optimization of a flow cytometry protocol for detection and viability assessment of *Giardia lamblia*. Travel. Med. Infect. Dis. **6**(4), 234–239 (2008)
40. J.M. Barbosa, S. Costa-de-Oliveira, A.G. Rodrigues, T. Hanscheid, H. Shapiro, C. Pina-Vaz, A flow cytometric protocol for detection of *Cryptosporidium* spp. Cytometry A **73**(1), 44–47 (2008)
41. B.M. Hsu, N.M. Wu, H.D. Jang, F.C. Shih, M.T. Wan, C.M. Kung, Using the flow cytometry to quantify the *Giardia* cysts and *Cryptosporidium* oocysts in water samples. Environ. Monit. Assess. **104**(1–3), 155–162 (2005).
42. C. Sakamoto, N. Yamaguchi, M. Yamada, H. Nagase, M. Seki, M. Nasu, Rapid quantification of bacterial cells in potable water using a simplified microfluidic device. J. Microbiol. Methods. **68**(3), 643–647 (2007)
43. D. McDougald, S.A. Rice, D. Weichart, S. Kjelleberg, Nonculturability: adaptation or debilitation? FEMS Microbiol. Ecol. **25**(1), 1–9 (1998).
44. H. Strauber, S. Muller, Viability states of bacteria–specific mechanisms of selected probes. Cytometry A **77**(7), 623–634 (2010).
45. C.P. Brussaard, D. Marie, G. Bratbak, Flow cytometric detection of viruses. J. Virol. Methods. **85**(1–2), 175–182 (2000).
46. E. Engvall, P. Perlmann, Enzyme-linked immunosorbent assay (ELISA). Quantitative assay of immunoglobulin G. Immunochemistry **8**(9), 871–874 (1971)
47. B.K. Van Weemen, A.H. Schuurs, Immunoassay using antigen-enzyme conjugates. FEBS Lett. **15**(3), 232–236 (1971)
48. D.A. Kulesh, D.R. Clive, D.S. Zarlenga, J.J. Greene, Identification of interferon-modulated proliferation-related cDNA sequences. Proc. Natl. Acad. Sci. U. S. A. **84**(23), 8453–8457 (1987)
49. M. Schena, D. Shalon, R.W. Davis, P.O. Brown, Quantitative monitoring of gene expression patterns with a complementary DNA microarray. Science **270**(5235), 467–470 (1995)
50. O. Nahshol, V. Bronner, A. Notcovich, L. Rubrecht, D. Laune, T. Bravman, Parallel kinetic analysis and affinity determination of hundreds of monoclonal antibodies using the ProteOn XPR36. Anal. Biochem. **383**(1), 52–60 (2008).
51. M.J. Linman, A. Abbas, Q. Cheng, Interface design and multiplexed analysis with surface plasmon resonance (SPR) spectroscopy and SPR imaging. Analyst **135**(11), 2759–2767 (2010)
52. F. Chowdhury, A. Williams, P. Johnson, Validation and comparison of two multiplex technologies, Luminex® and Mesoscale Discovery, for human cytokine profiling. J. Immunol. Methods **340**(1), 55–64 (2009).
53. EMD Millipore, Human cytokine/chemokine panel http://www.millipore.com/userguides.nsf/a73664f9f981af8c852569b9005b4eee/506688139fe4c9a98525742c007755db/$FILE/MPXHCYTO-60K.pdf, (2011).

54. EMD Millipore, Human cytokine/chemokine magnetic bead panel http://www.millipore.com/userguides.nsf/a73664f9f981af8c852569b9005b4eee/e1dbeddc233bfd438525767f00679241/$FILE/HCYTOMAG-60K.MPX.pdf, (2011).
55. luminex xMAP® technology http://www.luminexcorp.com/TechnologiesScience/xMAPTechnology/index.htm, (2011).